1   **The neonatal microenvironment programs conventional and intestinal**

2   **Tbet+ γδT17 cells through the transcription factor STAT5**

3   Darshana Kadekar[1]*, Rasmus Agerholm[1]*, John Rizk[1]*, Heidi Neubauer[2], Tobias Suske[2], Barbara

4   Maurer[2], Monica Torrellas Viñals[1], Elena Comelli[3], Amel Taibi[3], Richard Moriggl[2,4,5] and Vasileios

5   Bekiaris[1]#

6   [1]Department of Health Technology, Technical University of Denmark, Kemitorvet, Bldg 202, 2800

7   Kgs Lyngby, Denmark.

8   [2]Institute of Animal Breeding and Genetics, University of Veterinary Medicine Vienna, 1210 Vienna,

9   Austria.

10   [3]Department of Nutritional Sciences, University of Toronto, Toronto, ON, M5S 1A8

11   [4]Medical University of Vienna, 1090 Vienna, Austria.

12   [5]Ludwig Boltzmann Institute for Cancer Research, 1090 Vienna, Austria.

13   * equal contributing authors; # corresponding author (vasbek@dtu.dk)

14

15   **Summary**

16   Interleukin(IL)-17-producing RORγt+ γδ T (γδT17) cells develop in the embryonic thymus and

17   participate in type 3 immune responses. Herein we show that γδT17 cells rapidly proliferate within

18   neonatal lymph nodes and gut, where upon entry they uniquely upregulate Tbet and co-express IL-

19   17, IL-22 and interferon(IFN) γ in a STAT3 and retinoic acid dependent manner. Neonatal

20   expansion was halted in mice conditionally deficient in STAT5 and its loss resulted in γδT17 cell

21   depletion from all adult organs. Hyperactive STAT5 mutant mice showed that the STAT5A

22   homologue had a dominant role over STAT5B in promoting γδT17 cell expansion and

23   downregulating gut-associated Tbet. In contrast, STAT5B preferentially expanded IFNγ-producing

24   γδ populations. Importantly, mice lacking γδT17 cells due to STAT5 deficiency displayed a

25   profound resistance to experimental autoimmune encephalomyelitis. Our data identify for the first

26   time STAT5 as a key molecular checkpoint allowing γδT17 cells to pass through a critical neonatal

27   developmental window to acquire tissue-specific characteristics essential for infection and

28   autoimmunity.

1

Introduction

Interleukin(IL)-17 producing gamma delta (γδ) T cells (γδT17) are one of the major type 3 innate lymphocytes in the mouse, occupying the skin and most mucosal surfaces as well as secondary lymphoid organs. Their ability to constitutively produce IL-17 and to respond rapidly to cytokines like IL-7, IL-23 and IL-1β renders them as a critical part of innate immunity to infections (Cho et al., 2010; Conti et al., 2014) but also makes them highly pathogenic in a number of inflammatory models (Bekiaris et al., 2013; Michel et al., 2012; Sutton et al., 2009). Thus, both experimental autoimmune encephalomyelitis (EAE) and imiquimod (IMQ)-induced psoriasis require the presence of functional γδT17 cells (Bekiaris et al., 2013; Sutton et al., 2009). Similarly, tumor models have shown that γδT17 cells can have either protective (Wu et al., 2014) or pathogenic (Coffelt et al., 2015) roles depending on the nature of the cancer. In humans, although a unique innate γδT17 cell population has not been yet characterized, many groups have identified IL-17-producing γδ T cells in association with various disease states (Cai et al., 2011; Wu et al., 2014).

Genetic murine studies have shown that γδT17 cells develop in the embryonic thymus in a step-wise fashion, initially involving escape of epithelial selection (Turchinovich and Hayday, 2011), followed by the upregulation of a number of transcription factors, such as RORγt, SOX13 and cMAF, that regulate lineage commitment, specification and functional maturation (Malhotra et al., 2013; Zuberbuehler et al., 2019). Although T cell receptor (TCR) signaling is necessary for γδT17 cell development (Wencker et al., 2014), experimental evidence based on hypomorphic CD3 mice and anti-CD3/TCR antibody administration suggested that only weak TCR signals are required (Munoz-Ruiz et al., 2016; Sumaria et al., 2017). In addition, a recent study showed that TCR signaling is not important for lineage specification but for transition into the early immature stage (Spidale et al., 2018). γδT17 cell generation is restricted to the embryonic and neonatal thymus (Haas et al., 2012) with the bone marrow displaying low capacity to produce these cells (Cai et al., 2014).

STAT transcription factors act downstream of cytokine and growth factor receptors to regulate a plethora of key biological processes, including lymphocyte development and function (Stark and Darnell, 2012). STAT5 is encoded by two genes, *Stat5a* and *Stat5b*, giving rise to two highly

2

57 homologous proteins with largely overlapping functions in mediating transcription of target genes,

58 although STAT5B has a more dominant role in lymphoid cells as well as in cancer progression (de

59 Araujo ED, 2019; Villarino et al., 2016). Mice deficient in both STAT5A and STAT5B have

60 increased perinatal mortality and lack or display a severe reduction in many lymphocytic

61 populations, such as αβ T, γδ T, regulatory CD4$^+$ T cells (Treg), natural killer (NK) T, NK and also

62 B cells (Hoelbl et al., 2006; Yao et al., 2006; Yao et al., 2007). Although mice deficient in either

63 STAT5A or STAT5B show hampered development and function of a few major lymphocyte

64 subsets, their phenotype is milder than the combined loss of the two isoforms (Imada et al., 1998;

65 Villarino et al., 2016; Villarino et al., 2017). However, there is currently no mechanistic data

66 regarding their individual contribution in γδ T cell biology. One of the suggested mechanisms for

67 the dependence of developing γδ T cell progenitors on STAT5 is its ability to induce TCRγ

68 rearrangements, due to three highly interspecies conserved inverted repeat STAT5 consensus

69 sites within the *TCRγ* locus (Wagatsuma et al., 2015).

70   In humans, *STAT5*-associated loss of function mutations are predominantly restricted to

71 STAT5B and these culminate in growth failure, due to impaired growth hormone receptor signaling,

72 as well as immunodeficiency, metabolic dysregulation and autoimmune disorders as a result of

73 Treg deficiency (Cohen et al., 2006; Hwa, 2016; Kanai et al., 2012). In contrast, *STAT5B* gain of

74 function (GOF) mutations strongly correlate with mature T cell neoplasms (Pham et al., 2018) and

75 have also been found in patients with neutrophilia or eosinophilia (Cross et al., 2019; Ma et al.,

76 2017). In particular, the recurrent N642H GOF missense mutation within the Src homology 2 (SH2)

77 domain of STAT5B results in enhanced and prolonged tyrosine phosphorylation (pY) in response

78 to low doses of cytokines or growth factors, and is associated with poorer patient prognosis and

79 increased risk of relapse (Bandapalli et al., 2014; Pham et al., 2018; Rajala et al., 2013).

80 Interestingly, *STAT5B* GOF mutations are relatively frequent in aggressive γδ T cell lymphoma

81 subtypes, such as hepatosplenic T cell lymphoma (Nicolae et al., 2014), monomorphic

82 epitheliotropic intestinal T cell lymphoma (Kucuk et al., 2015; Nairismagi et al., 2016) and primary

83 cutaneous γδ T cell lymphoma (Kucuk et al., 2015). Notably, approximately 20% of identified

84 N642H mutations occur in γδ T cell derived lymphomas (de Araujo ED, 2019).

3

85   Herein, we show that STAT5 is critically required for the progression and expansion of γδT17

86   cells through neonatal life in the intestine and periphery. We provide evidence that intestinal γδT17

87   cells upregulate Tbet upon entry into the lamina propria after birth and co-express the cytokines IL-

88   17, IL-22 and IFNγ in a mechanism dependent on STAT3 and retinoic acid. Furthermore, loss of

89   γδT17 cells due to STAT5 deficiency results in resistance to experimental autoimmune

90   encephalomyelitis in adult mice. Importantly, we show that STAT5A promotes γδT17 cell

91   expansion and downregulates intestinal Tbet favoring a type 17 program, whereas STAT5B favors

92   IFNγ-producing γδ populations and increases intestinal Tbet expression. Collectively, our data

93   suggest that neonatal life is a critical window of development and tissue specification for γδT17

94   cells, and that this process is tightly regulated by STAT5.

95

96   **Results**

97   **STAT5 regulates the neonatal expansion of γδT17 cells**

98   In order to test the importance of STAT5 in RORγt expressing γδ T cells, we crossed RORγt-Cre

99   mice (Eberl and Littman, 2004) with mice floxed for both STAT5a and STAT5b (RORγt^{CRE}-

100   STAT5$^{F/F}$) (Cui et al., 2004) and analyzed the numbers of LN and skin γδT17 cells. We found that

101   compared to littermate controls (Cre$^-$), RORγt^{CRE}-STAT5$^{F/F}$ mice (Cre$^+$) contained severely reduced

102   numbers of γδT17 cells defined phenotypically as CD27$^-$CD44$^+$ in the LN and CCR6$^+$CD3$^+$ in the

103   skin (Fig. 1A-B). This was confirmed by the near complete lack of IL-17-expressing γδ T cells in

104   the LN (Fig. 1C). Deficiency in STAT5 equally affected both Vγ4$^+$ and Vγ4$^-$ subsets of γδT17 cells

105   (not shown). Interestingly, RORγt^{CRE}-STAT5$^{F/F}$ mice had a concomitant increase in IFNγ-

106   expressing γδ T cells (Fig. 1C). In RORγt^{CRE}-STAT5$^{F/F}$ mice, deletion of STAT5 in CD4$^+$ and CD8$^+$

107   T cells was not complete (Fig. S1A). Insufficient deletion in the αβ T cell compartment using

108   RORγt^{CRE} deleter mice has also been demonstrated by others (Guo et al., 2014). Consequently,

109   we did not observe differences in the numbers of TCRβ$^+$CD4$^+$CCR6$^+$ cells, which are enriched for

110   T-helper-17 (Th17) cells (Fig S1B), or in the frequency of IFNγ-producing CD4$^+$ T cells (Fig S1B).

111   Surprisingly, and also in agreement with previous observations (Laurence et al., 2007), the

112   percentage of IL-17A-producing CD4$^+$ T cells was higher even when STAT5 was only partially

4

113 deleted (Fig. S1B). Finally, to determine whether the defect we observed in RORγt[CRE]-STAT5[F/F]

114 mice was intrinsic to the γδT17 population we generated mixed bone marrow chimeras using

115 CD45.1[+] wild-type and Cre[+] CD45.2[+] donors and analyzed lymph nodes and skin 12 weeks later.

116 We found that by comparison to wild-type, RORγt[CRE]-STAT5[F/F] BM failed to generate γδT17 cells

117 suggesting that the STAT5-associated defect is cell intrinsic (Fig. S2A). It is noteworthy that in the

118 skin we could not detect any γδT17 cells originating from RORγt[CRE]-STAT5[F/F] BM (Fig. S2A).

119 We next investigated whether reduced γδT17 cell numbers in the absence of STAT5 were due

120 to a developmental defect. We therefore examined newborn thymi from RORγt[CRE]-STAT5[F/F] and

121 littermate control mice and found no differences in γδT17 cellularity (Fig. 1D) or IL-17A expression

122 (Fig. S2B). Expression of both *Stat5a* and *Stat5b* was significantly lower in RORγt[CRE]-STAT5[F/F]

123 γδT17 cells sorted from new born thymi compared to Cre^{−} controls or CD27^{+} γδ T cells (Fig. S2C).

124 This suggested that the major impact of STAT5 occurs extrathymically. We thus analyzed neonatal

125 mice and found a significant decrease in LN γδT17 cell numbers in 7 and 14 day old mice (Fig.

126 1E). Assessment of proliferation by Ki67 staining showed that γδT17 cells in RORγt[CRE]-STAT5[F/F]

127 neonatal mice displayed reduced turnover compared to controls (Fig. 1F). Furthermore, expression

128 of the anti-apoptotic STAT5 target gene product BCL2 (Tripathi et al., 2010; Yao et al., 2006) was

129 reduced in neonatal STAT5-deficient γδT17 cells (Fig. S2D), suggesting impaired survival.

130 Collectively, we demonstrate that STAT5 is important for the turnover and survival of γδT17 cells

131 during neonatal and adult life.

132

133 **Differential regulation of γδT17 and CD27^{+} γδ T cells by STAT5A and STAT5B**

134 Since deficiency in STAT5 resulted in near complete loss of γδT17 cells, we next examined the

135 influence of hyperactive STAT5 expression. We utilized two established models of STAT5

136 hyperactivity whereby the *Vav1* promoter drives the expression of (a) high or low copies of the

137 hyperactive S710F STAT5A mutant (Maurer et al., 2019; Onishi et al., 1998), or (b) human wild-

138 type (WT) or the hyperactive N642H STAT5B mutant (Pham et al., 2018). Constitutively high levels

139 of hyperactive STAT5A resulted in very high numbers of γδT17 cells in LN, but hyperactivation of

140 STAT5A had a considerably smaller impact on CD27^{+} γδ T cells (Fig. 2A-B). In contrast,

141 constitutive expression of hyperactive STAT5B increased the numbers of CD27$^+$ γδ T but had a

142 smaller effect on γδT17 cells (Fig. 2A-B). When we analyzed cytokine expression we found that

143 IFNγ was only induced by hyperactive STAT5B (Fig. S2E), whereas IL-17A could be induced at

144 high levels both by hyperactive STAT5A as well as WT STAT5B expression (Fig. 2C). However,

145 hyperactive STAT5B did not induce IL-17A expression (Fig. 2C).

146   Similar to the LN, skin γδT17 cell numbers were greatly enhanced by hyperactive STAT5A

147 whereas STAT5B had a milder impact (Fig. 2D-E). With the exception of Vγ5$^+$ dendritic epidermal

148 T cells, CCR6$^+$ γδT17 cells are the only γδ population in the skin. However, mice expressing

149 hyperactive STAT5B, and to a lesser extent mice expressing hyperactive STAT5A, contained

150 CCR6$^-$ γδ T cells that were either Vγ4$^+$ or Vγ4$^-$ (Fig. 2D-F). Collectively, our data pinpoint towards

151 a dominant role of STAT5A in supporting γδT17 cells in LN and skin, with STAT5B supporting

152 mainly IFNγ-producing and CCR6$^-$ γδ T cells.

153

154 **RORγt^{CRE}-STAT5$^{F/F}$ mice are resistant to experimental autoimmune encephalomyelitis**

155 γδT17 cells have been implicated in the pathogenesis of experimental autoimmune

156 encephalomyelitis (EAE) (Petermann et al., 2010; Sutton et al., 2009) and we therefore

157 investigated how well RORγt^{CRE}-STAT5$^{F/F}$ mice responded to MOG (myelin oligodendrocyte

158 glycoprotein)-induced EAE. We found that compared to littermate controls, RORγt^{CRE}-STAT5$^{F/F}$

159 mice were resistant to EAE symptoms (Fig. 3A). This correlated with significantly reduced γδT17

160 cells in the LN and brain at days 11 and 21 after immunization (Fig. 3B-D). As expected, γδ T cell

161 associated IL-17A production was significantly reduced at all time points in mice lacking STAT5

162 (Fig. 3E). Although it has been recently suggested that inflammatory conditions during EAE can *de*

163 *novo* regenerate γδT17 cells (Papotto et al., 2017a), our data suggest that in the absence of

164 STAT5, γδT17 cell regeneration cannot occur.

165   It has been shown that in addition to their direct contribution to EAE pathogenesis, γδT17 cells

166 are required for optimal Th17 responses (Sutton et al., 2009). We therefore interrogated the CD4$^+$

167 T cell response in the LN and brain of RORγt^{CRE}-STAT5$^{F/F}$ and littermate control mice during EAE.

168 We found that the numbers and cytokine production of CD4$^+$ T cells were not affected in the LN

169   (Fig. S1C-D), which may be a reflection of the levels of STAT5 still detectable in these cells (Fig.

170   S1A). As expected from the clinical score and the lack of pro-inflammatory γδT17 cells, there was

171   a profound reduction in CD4$^+$ T cell numbers within the brain of RORγt^{CRE}-STAT5$^{F/F}$ mice (Fig. 3F).

172   Collectively, our data show that loss of γδT17 cells due to STAT5 deficiency is associated with

173   dramatically reduced inflammatory responses in the EAE model.

174

175   **Intestinal lamina propria γδT17 cells express Tbet and require STAT3 and retinoic acid for**

176   **cytokine production**

177   Besides the skin and peripheral lymphoid tissues, γδ T cells with type 3 functionality have been

178   described in the mucosa such as the lung and gut (Sheridan et al., 2013; Sutherland et al., 2014).

179   We therefore wanted to test whether STAT5 regulated γδT17 cells specifically in the intestinal

180   lamina propria (LP). In order to avoid potential differences in γδT17 surface markers in the gut, we

181   stained small intestinal and colonic LP (sLP and cLP respectively) for RORγt and Tbet and

182   compared this to peripheral LNs. Surprisingly, we found that many RORγt$^+$ γδ T cells in the gut co-

183   expressed Tbet (Fig. 4A). We additionally confirmed the presence of RORγt$^+$Tbet$^+$ γδ T cells by

184   generating double transgenic mice reporting GFP and AmCyan under control of the promoters for

185   RORγt and Tbet, respectively (Fig S3A). By transcription factor staining analysis we found that the

186   RORγt$^+$Tbet$^+$ γδ T cell population was more prevalent in the ileum and proximal colon (Fig. 4B),

187   which contrasted with the distribution of RORγt$^-$Tbet$^+$ γδ T cells in the same locations (Fig. S3B).

188   In order to investigate which factors regulate the expression of Tbet, we analyzed mice deficient in

189   Toll-like receptor and IL-12 signaling as well as mice depleted of their intestinal microbial flora. We

190   found that expression of Tbet was independent of the microbiota (Fig. S3C), MyD88, TRIF and IL-

191   12 signaling (Fig. S3D).

192   In agreement with their innate nature, intestinal γδT17 cells produced IL-17A, IL-22 and IFNγ

193   as early as 7 days after birth (Fig. 4C), indicating a functional γδT17 population that has acquired

194   the ability to produce IFNγ at steady-state. Using RORγt^{CRE}-STAT3$^{F/F}$ mice, we showed that

195   production of both IL-17A and IL-22 was STAT3-dependent (Fig. 4D-E and S4A-B). One of the key

196   factors regulating IFNγ-expressing cells is retinoic acid (RA) (Brown et al., 2015). We therefore

197   interrogated mice possessing a RA receptor (RAR) dominant negative (RARdn) transgene, which

198   prevents active RARα signaling (Rajaii et al., 2008) in RORγt-expressing cells (RORγt^CRE-

199   RARdn^F/F mice). We found that loss of RA signaling was associated with reduced overall

200   expression of IFNγ (Fig. 5A and S4C) as well as reduced frequency of IL-17A^+IFNγ^+ and IL-

201   22^+IFNγ^+ cells (Fig. 5B and S4D). In contrast, deficiency in RA signaling resulted in significantly

202   increased frequency of IL-17A^+IFNγ^− and IL-22^+IFNγ^− Tbet^+ γδT17 cells in the colon and small

203   intestine (Fig. 5B and S4D). Collectively, this data indicates that lamina propria Tbet^+ γδT17 cells

204   are innate cells that can co-produce IL-17, IL-22 and IFNγ, and that their cytokine expression

205   profile is regulated by STAT3 and RA.

206

207   **STAT5 regulates Tbet expression and determines the progression of intestinal γδT17 cells**

208   **through neonatal development**

209   Following the identification of a distinct gut-specific γδT17 population, we aimed to understand

210   their dependence on STAT5. Similar to LNs, RORγt-expressing γδ T cells, irrespective of Tbet,

211   were drastically and significantly reduced from the sLP and cLP of RORγt^CRE-STAT5^F/F mice (Fig.

212   6A-B). Analysis of GOF STAT5A and STAT5B mice revealed that hyperactive STAT5A

213   downregulated Tbet in RORγt^+ cLP γδ T cells, whereas hyperactive STAT5B enhanced it (Fig. 6C)

214   suggesting a YIN/YANG regulation in RORγt^+ cLP γδ T cells by STAT5A versus STAT5B.

215   Hyperactive STAT5A preferentially expanded RORγt^+ cells in the gut whereas hyperactive

216   STAT5B favored Tbet-expressing γδ T cells irrespective of whether they expressed RORγt or not

217   (Fig. 6D-F).

218   Next, we sought to determine whether STAT5 also regulated RORγt^+Tbet^+ γδ T cells

219   neonatally. We therefore analyzed neonatal gut at different time points and found that 1-2 days

220   after birth γδ T cells in the colon and small intestine expressed either RORγt or Tbet but not both

221   (Fig. 7A-C and S5A-C). Tbet was induced in RORγt-expressing cells at day 4 and stabilized to

222   adult levels within the first week of life (Fig. 7A-B and S5A-B). Expression of Tbet at neonatal day 4

223   coincided with a rapid increase in cell proliferation, which was blunted in the absence of STAT5

224   (Fig. 7D and S5D). RORγt^CRE-STAT5^F/F mice did not upregulate Tbet and failed to sustain a

225   RORγt$^+$ γδ T cell population after birth (Fig. 7A-C and S5A-C). However, despite their functional

226   presence in the neonatal gut, RORγt-expressing γδ T cells were not necessary for protection

227   against early life infection with the attaching and effacing bacterium *Citrobacter rodentium* (Fig.

228   S6A-C).

229   Collectively, our data demonstrate that during neonatal life STAT5 acts as a molecular

230   checkpoint to promote proliferation of intestinal γδT17 cells. Moreover, our data reveal an

231   interesting balance between STAT5A and STAT5B, which appear to have opposing roles in the

232   regulation of Tbet expression, thereby differentially coordinating tissue specificity of γδT17 cells.

233

234   **Discussion**

235   In the present study we demonstrate that STAT5 is a critical regulator of IL-17-producing γδ T cells

236   in the periphery, skin and gut. STAT5 was necessary during neonatal life in order to sustain

237   proliferation and survival of γδT17 cells. Transgenic reconstitution of hyperactive STAT5 variants

238   showed that STAT5A preferentially sustains γδT17 whereas STAT5B promotes IFNγ-producing γδ

239   T cells. Physiologically, hampered development of γδT17 cells due to STAT5 loss resulted in near

240   complete resistance to EAE pathology and prevented Th17 cells from infiltrating the brain.

241   Furthermore, we discovered that intestinal lamina propria γδT17 cells co-express the type 1

242   transcription factor Tbet and can produce IL-17, IL-22 and IFNγ in a STAT3- and RA-dependent

243   mechanism. Intestinal γδT17 cells upregulate Tbet during the first week of life and are strictly

244   STAT5-dependent for their neonatal development. Furthermore, expression of Tbet is under the

245   antagonistic control of STAT5A and STAT5B.

246   STAT5 is a major signaling component downstream of many cytokine and growth factor

247   receptors and is therefore involved in the development of lymphocyte lineages (Rani and Murphy,

248   2016). Hence, both mice and humans with STAT5-associated deficiencies are severely

249   immunocompromized (Imada et al., 1998; Kofoed et al., 2003). T cells of the γδ lineage are

250   reduced in the thymus and lymphoid tissues of full STAT5-deficient mice (Hoelbl et al., 2006), and

251   this has been attributed to a failure to successfully rearrange the TCR early during embryonic

252   development (Wagatsuma et al., 2015). However, our data show that γδT17 cells require STAT5

9

253 signaling to expand and survive after they exit the thymus. This suggests that γδ T cell subsets rely

254 on STAT5 during different steps of their development and differentiation, presumably reflecting

255 cytokine niches within the local microenvironment.

256   Detailed molecular and phenotypic studies utilizing mice deficient in either STAT5A or

257 STAT5B have shown that despite their many commonalties, particularly at the genome-wide level,

258 the two STAT5 gene products can display cell-specific functions (Villarino et al., 2016; Villarino et

259 al., 2017). Thus, in CD4$^+$ T cells STAT5B has a dominant role in orchestrating differentiation and

260 function. In this regard, our data show that both STAT5A and STAT5B can have dominant and

261 differential roles in γδ T cells depending on the specific subset. Whereas STAT5A regulated almost

262 exclusively γδT17 cells and downregulated intestinal Tbet expression, STAT5B had a prevailing

263 effect on IFNγ-expressing γδ populations. This suggests that unlike in CD4$^+$ helper and innate

264 lymphoid cells, STAT5A and STAT5B display significant, differential regulatory functions in γδ T

265 cell subsets, and further pinpoints to the distinct molecular, functional and developmental

266 requirements of γδT17 compared to non-IL-17-producing subsets. The unique roles that we

267 uncovered herein for STAT5A and STAT5B suggest that they display cell-specific functions and

268 can have context-dependent, non-redundant roles in generating robust immune responses. The

269 genetic and cellular tools that we used herein will be crucial to illuminate the specific biological

270 functions of these two highly species-conserved proteins that play indispensable roles in infection,

271 cancer and autoimmunity.

272   Although γδT17 cells develop in the embryonic thymus, previous reports suggested that they

273 populate the skin and LNs after birth (Cai et al., 2014). Findings herein indicate that the neonatal

274 period is critical for γδT17 cells to populate lymphoid and non-lymphoid tissues. A critical time

275 window of opportunity has been suggested to exist during neonatal life when, upon exposure to

276 microbiota, the immune system matures and develops cellular and humoral immunity (Al Nabhani

277 et al., 2019; Torow and Hornef, 2017). The upregulation of Tbet in murine intestinal γδT17 cells

278 within days after birth and its independence on the microbiota and TLR signals suggests

279 alternative neonatal factors such as lactation, which is predominantly STAT5A-controlled

280 (Haricharan and Li, 2014). Neonatal-specific cytokine milieus that activate STAT5 may also

10

281 regulate Tbet expression in the developing gut. In this regard, hyperactive STAT5A downregulated

282 Tbet whereas high STAT5B activity induced it, although whether this was direct or indirect through

283 regulation of cell fate transcriptional regulators remains to be studied. Nevertheless, the

284 identification of Tbet-expressing γδT17 cells at steady-state indicates a form of plasticity within this

285 lineage that is regulated post-thymically and in a tissue-specific manner. The importance of Tbet in

286 γδT17 cells is currently unknown. However, the co-expression of IFNγ suggests that acquisition of

287 type 1 transcriptional and functional traits may give an advantage over infection, similar to innate

288 lymphoid cells and Th1-transitioning Th17 cells.

289   Animal models have linked γδT17 cells to immune responses during inflammation, infection

290 and cancer where they can be either protective or pathogenic (Papotto et al., 2017b). In the

291 imiquimod model of psoriasis, γδT17 cells are important to drive disease; however, their

292 pathogenic role can be redundant and compensated by other inflammatory cells (Sandrock et al.,

293 2018). In the EAE mouse model, γδT17 cells have also been shown to contribute to pathogenicity

294 (Petermann et al., 2010; Sutton et al., 2009). Herein, we provide evidence that γδT17 cells are

295 necessary and non-redundant for full development of EAE symptoms and for the mobilization of

296 Th17 cells to the brain. Despite their absence from all major organs from neonatal life onwards,

297 other innate inflammatory cells could not compensate for their absence. γδ T cells have co-evolved

298 alongside αβ T and B cells (Hirano et al., 2013), however their function has diversified and was

299 imprinted by the specific tissue cues present in different locations. It is thus not surprising that the

300 immunological response of different γδ T cell subsets will vary and will be essential or redundant

301 depending on the inflammatory or infectious context.

302   In summary, we provide evidence that the neonatal microenvironment, acting in synergy with

303 tissue-specific and STAT5-driven molecular cues, regulates the development, functional

304 maturation and immunological importance of γδT17 cells.

305

306 **References**

307 Al Nabhani, Z., Dulauroy, S., Marques, R., Cousu, C., Al Bounny, S., Dejardin, F., Sparwasser, T.,
308 Berard, M., Cerf-Bensussan, N., and Eberl, G. (2019). A Weaning Reaction to Microbiota Is
309 Required for Resistance to Immunopathologies in the Adult. Immunity.

310 Bandapalli, O.R., Schuessele, S., Kunz, J.B., Rausch, T., Stutz, A.M., Tal, N., Geron, I.,
311 Gershman, N., Izraeli, S., Eilers, J., *et al.* (2014). The activating STAT5B N642H mutation is a
312 common abnormality in pediatric T-cell acute lymphoblastic leukemia and confers a higher risk of
313 relapse. Haematologica *99*, e188-192.

315 Bekiaris, V., Sedy, J.R., Macauley, M.G., Rhode-Kurnow, A., and Ware, C.F. (2013). The Inhibitory
316 Receptor BTLA Controls gammadelta T Cell Homeostasis and Inflammatory Responses. Immunity
317 *39*, 1082-1094.

319 Brown, C.C., Esterhazy, D., Sarde, A., London, M., Pullabhatla, V., Osma-Garcia, I., Al-Bader, R.,
320 Ortiz, C., Elgueta, R., Arno, M., *et al.* (2015). Retinoic acid is essential for Th1 cell lineage stability
321 and prevents transition to a Th17 cell program. Immunity *42*, 499-511.

323 Cai, Y., Shen, X., Ding, C., Qi, C., Li, K., Li, X., Jala, V.R., Zhang, H.G., Wang, T., Zheng, J., and
324 Yan, J. (2011). Pivotal role of dermal IL-17-producing gammadelta T cells in skin inflammation.
325 Immunity *35*, 596-610.

327 Cai, Y., Xue, F., Fleming, C., Yang, J., Ding, C., Ma, Y., Liu, M., Zhang, H.G., Zheng, J., Xiong, N.,
328 and Yan, J. (2014). Differential developmental requirement and peripheral regulation for dermal
329 Vgamma4 and Vgamma6T17 cells in health and inflammation. Nature communications *5*, 3986.

331 Cho, J.S., Pietras, E.M., Garcia, N.C., Ramos, R.I., Farzam, D.M., Monroe, H.R., Magorien, J.E.,
332 Blauvelt, A., Kolls, J.K., Cheung, A.L., *et al.* (2010). IL-17 is essential for host defense against
333 cutaneous Staphylococcus aureus infection in mice. J Clin Invest *120*, 1762-1773.

335 Coffelt, S.B., Kersten, K., Doornebal, C.W., Weiden, J., Vrijland, K., Hau, C.S., Verstegen, N.J.M.,
336 Ciampricotti, M., Hawinkels, L., Jonkers, J., and de Visser, K.E. (2015). IL-17-producing
337 gammadelta T cells and neutrophils conspire to promote breast cancer metastasis. Nature *522*,
338 345-348.

340 Cohen, A.C., Nadeau, K.C., Tu, W., Hwa, V., Dionis, K., Bezrodnik, L., Teper, A., Gaillard, M.,
341 Heinrich, J., Krensky, A.M., *et al.* (2006). Cutting edge: Decreased accumulation and regulatory
342 function of CD4+ CD25(high) T cells in human STAT5b deficiency. J Immunol *177*, 2770-2774.

344 Conti, H.R., Peterson, A.C., Brane, L., Huppler, A.R., Hernandez-Santos, N., Whibley, N., Garg,
345 A.V., Simpson-Abelson, M.R., Gibson, G.A., Mamo, A.J., *et al.* (2014). Oral-resident natural Th17
346 cells and gammadelta T cells control opportunistic Candida albicans infections. J Exp Med *211*,
347 2075-2084.

349 Cross, N.C.P., Hoade, Y., Tapper, W.J., Carreno-Tarragona, G., Fanelli, T., Jawhar, M., Naumann,
350 N., Pieniak, I., Lubke, J., Ali, S., *et al.* (2019). Recurrent activating STAT5B N642H mutation in
351 myeloid neoplasms with eosinophilia. Leukemia *33*, 415-425.

353 Cui, Y., Riedlinger, G., Miyoshi, K., Tang, W., Li, C., Deng, C.X., Robinson, G.W., and
354 Hennighausen, L. (2004). Inactivation of Stat5 in mouse mammary epithelium during pregnancy
355 reveals distinct functions in cell proliferation, survival, and differentiation. Mol Cell Biol *24*, 8037-
356 8047.

358 de Araujo ED, E.F., Neubauer HA, Meneksedag-Erol D, Manaswiyoungkul P, Eram MS, Seo H,
359 Qadree AK, Israelian J, Orlova A, Suske T, Pham HTT, Boersma A, Tangermann S, Kenner L,
360 Rülicke T, Dong A, Ravichandran M, Brown PJ, Audette GF, Rauscher S, Dhe-Paganon S, Moriggl
361 R, Gunning PT (2019). Structural and Functional Consequences of the STAT5BN642H Driver
362 Mutation. Nature communications.

364 Eberl, G., and Littman, D.R. (2004). Thymic origin of intestinal alphabeta T cells revealed by fate
365 mapping of RORgammat+ cells. Science *305*, 248-251.

366 Guo, X., Qiu, J., Tu, T., Yang, X., Deng, L., Anders, R.A., Zhou, L., and Fu, Y.X. (2014). Induction
367 of innate lymphoid cell-derived interleukin-22 by the transcription factor STAT3 mediates protection
368 against intestinal infection. Immunity *40*, 25-39.

370 Haas, J.D., Ravens, S., Duber, S., Sandrock, I., Oberdorfer, L., Kashani, E., Chennupati, V.,
371 Fohse, L., Naumann, R., Weiss, S.*, et al.* (2012). Development of interleukin-17-producing
372 gammadelta T cells is restricted to a functional embryonic wave. Immunity *37*, 48-59.

374 Haricharan, S., and Li, Y. (2014). STAT signaling in mammary gland differentiation, cell survival
375 and tumorigenesis. Mol Cell Endocrinol *382*, 560-569.

377 Hirano, M., Guo, P., McCurley, N., Schorpp, M., Das, S., Boehm, T., and Cooper, M.D. (2013).
378 Evolutionary implications of a third lymphocyte lineage in lampreys. Nature *501*, 435-438.

380 Hoelbl, A., Kovacic, B., Kerenyi, M.A., Simma, O., Warsch, W., Cui, Y., Beug, H., Hennighausen,
381 L., Moriggl, R., and Sexl, V. (2006). Clarifying the role of Stat5 in lymphoid development and
382 Abelson-induced transformation. Blood *107*, 4898-4906.

384 Hwa, V. (2016). STAT5B deficiency: Impacts on human growth and immunity. Growth Horm IGF
385 Res *28*, 16-20.

387 Imada, K., Bloom, E.T., Nakajima, H., Horvath-Arcidiacono, J.A., Udy, G.B., Davey, H.W., and
388 Leonard, W.J. (1998). Stat5b is essential for natural killer cell-mediated proliferation and cytolytic
389 activity. J Exp Med *188*, 2067-2074.

391 Kanai, T., Jenks, J., and Nadeau, K.C. (2012). The STAT5b Pathway Defect and Autoimmunity.
392 Frontiers in immunology *3*, 234.

394 Kofoed, E.M., Hwa, V., Little, B., Woods, K.A., Buckway, C.K., Tsubaki, J., Pratt, K.L., Bezrodnik,
395 L., Jasper, H., Tepper, A.*, et al.* (2003). Growth hormone insensitivity associated with a STAT5b
396 mutation. N Engl J Med *349*, 1139-1147.

398 Kucuk, C., Jiang, B., Hu, X., Zhang, W., Chan, J.K., Xiao, W., Lack, N., Alkan, C., Williams, J.C.,
399 Avery, K.N.*, et al.* (2015). Activating mutations of STAT5B and STAT3 in lymphomas derived from
400 gammadelta-T or NK cells. Nature communications *6*, 6025.

402 Laurence, A., Tato, C.M., Davidson, T.S., Kanno, Y., Chen, Z., Yao, Z., Blank, R.B., Meylan, F.,
403 Siegel, R., Hennighausen, L.*, et al.* (2007). Interleukin-2 signaling via STAT5 constrains T helper
404 17 cell generation. Immunity *26*, 371-381.

406 Lochner, M., Peduto, L., Cherrier, M., Sawa, S., Langa, F., Varona, R., Riethmacher, D., Si-Tahar,
407 M., Di Santo, J.P., and Eberl, G. (2008). In vivo equilibrium of proinflammatory IL-17+ and
408 regulatory IL-10+ Foxp3+ RORgamma t+ T cells. J Exp Med *205*, 1381-1393.

410 Ma, C.A., Xi, L., Cauff, B., DeZure, A., Freeman, A.F., Hambleton, S., Kleiner, G., Leahy, T.R.,
411 O'Sullivan, M., Makiya, M.*, et al.* (2017). Somatic STAT5b gain-of-function mutations in early onset
412 nonclonal eosinophilia, urticaria, dermatitis, and diarrhea. Blood *129*, 650-653.

414 Malhotra, N., Narayan, K., Cho, O.H., Sylvia, K.E., Yin, C., Melichar, H., Rashighi, M., Lefebvre, V.,
415 Harris, J.E., Berg, L.J.*, et al.* (2013). A network of high-mobility group box transcription factors
416 programs innate interleukin-17 production. Immunity *38*, 681-693.

418 Maurer, B., Nivarthi, H., Wingelhofer, B., Pham, H.T.T., Schlederer, M., Suske, T., Grausenburger,
419 R., Schiefer, A.I., Prchal-Murphy, M., Chen, D.*, et al.* (2019). High activation of STAT5A drives
420 peripheral T-cell lymphoma and leukemia. Haematologica.

Michel, M.L., Pang, D.J., Haque, S.F., Potocnik, A.J., Pennington, D.J., and Hayday, A.C. (2012). Interleukin 7 (IL-7) selectively promotes mouse and human IL-17-producing gammadelta cells. Proc Natl Acad Sci U S A *109*, 17549-17554.

Munoz-Ruiz, M., Ribot, J.C., Grosso, A.R., Goncalves-Sousa, N., Pamplona, A., Pennington, D.J., Regueiro, J.R., Fernandez-Malave, E., and Silva-Santos, B. (2016). TCR signal strength controls thymic differentiation of discrete proinflammatory gammadelta T cell subsets. Nat Immunol *17*, 721-727.

Nairismagi, M.L., Tan, J., Lim, J.Q., Nagarajan, S., Ng, C.C., Rajasegaran, V., Huang, D., Lim, W.K., Laurensia, Y., Wijaya, G.C.*, et al.* (2016). JAK-STAT and G-protein-coupled receptor signaling pathways are frequently altered in epitheliotropic intestinal T-cell lymphoma. Leukemia *30*, 1311-1319.

Nicolae, A., Xi, L., Pittaluga, S., Abdullaev, Z., Pack, S.D., Chen, J., Waldmann, T.A., Jaffe, E.S., and Raffeld, M. (2014). Frequent STAT5B mutations in gammadelta hepatosplenic T-cell lymphomas. Leukemia *28*, 2244-2248.

Onishi, M., Nosaka, T., Misawa, K., Mui, A.L., Gorman, D., McMahon, M., Miyajima, A., and Kitamura, T. (1998). Identification and characterization of a constitutively active STAT5 mutant that promotes cell proliferation. Mol Cell Biol *18*, 3871-3879.

Papotto, P.H., Goncalves-Sousa, N., Schmolka, N., Iseppon, A., Mensurado, S., Stockinger, B., Ribot, J.C., and Silva-Santos, B. (2017a). IL-23 drives differentiation of peripheral gammadelta17 T cells from adult bone marrow-derived precursors. EMBO Rep.

Papotto, P.H., Ribot, J.C., and Silva-Santos, B. (2017b). IL-17+ gammadelta T cells as kick-starters of inflammation. Nat Immunol *18*, 604-611.

Petermann, F., Rothhammer, V., Claussen, M.C., Haas, J.D., Blanco, L.R., Heink, S., Prinz, I., Hemmer, B., Kuchroo, V.K., Oukka, M., and Korn, T. (2010). gammadelta T cells enhance autoimmunity by restraining regulatory T cell responses via an interleukin-23-dependent mechanism. Immunity *33*, 351-363.

Pham, H.T.T., Maurer, B., Prchal-Murphy, M., Grausenburger, R., Grundschober, E., Javaheri, T., Nivarthi, H., Boersma, A., Kolbe, T., Elabd, M.*, et al.* (2018). STAT5BN642H is a driver mutation for T cell neoplasia. J Clin Invest *128*, 387-401.

Rajaii, F., Bitzer, Z.T., Xu, Q., and Sockanathan, S. (2008). Expression of the dominant negative retinoid receptor, RAR403, alters telencephalic progenitor proliferation, survival, and cell fate specification. Dev Biol *316*, 371-382.

Rajala, H.L., Eldfors, S., Kuusanmaki, H., van Adrichem, A.J., Olson, T., Lagstrom, S., Andersson, E.I., Jerez, A., Clemente, M.J., Yan, Y.*, et al.* (2013). Discovery of somatic STAT5b mutations in large granular lymphocytic leukemia. Blood *121*, 4541-4550.

Rani, A., and Murphy, J.J. (2016). STAT5 in Cancer and Immunity. J Interferon Cytokine Res *36*, 226-237.

Sagaidak, S., Taibi, A., Wen, B., and Comelli, E.M. (2016). Development of a real-time PCR assay for quantification of Citrobacter rodentium. J Microbiol Methods *126*, 76-77.

Sandrock, I., Reinhardt, A., Ravens, S., Binz, C., Wilharm, A., Martins, J., Oberdorfer, L., Tan, L., Lienenklaus, S., Zhang, B.*, et al.* (2018). Genetic models reveal origin, persistence and non-redundant functions of IL-17-producing gammadelta T cells. J Exp Med *215*, 3006-3018.

14

476 Sheridan, B.S., Romagnoli, P.A., Pham, Q.M., Fu, H.H., Alonzo, F., 3rd, Schubert, W.D., Freitag,
477 N.E., and Lefrancois, L. (2013). gammadelta T cells exhibit multifunctional and protective memory
478 in intestinal tissues. Immunity *39*, 184-195.
479
480 Spidale, N.A., Sylvia, K., Narayan, K., Miu, B., Frascoli, M., Melichar, H.J., Zhihao, W., Kisielow, J.,
481 Palin, A., Serwold, T.*, et al.* (2018). Interleukin-17-Producing gammadelta T Cells Originate from
482 SOX13(+) Progenitors that Are Independent of gammadeltaTCR Signaling. Immunity *49*, 857-872
483 e855.
484
485 Stark, G.R., and Darnell, J.E., Jr. (2012). The JAK-STAT pathway at twenty. Immunity *36*, 503-
486 514.
487
488 Sumaria, N., Grandjean, C.L., Silva-Santos, B., and Pennington, D.J. (2017). Strong
489 TCRgammadelta Signaling Prohibits Thymic Development of IL-17A-Secreting gammadelta T
490 Cells. Cell reports *19*, 2469-2476.
491
492 Sutherland, T.E., Logan, N., Ruckerl, D., Humbles, A.A., Allan, S.M., Papayannopoulos, V.,
493 Stockinger, B., Maizels, R.M., and Allen, J.E. (2014). Chitinase-like proteins promote IL-17-
494 mediated neutrophilia in a tradeoff between nematode killing and host damage. Nat Immunol *15*,
495 1116-1125.
496
497 Sutton, C.E., Lalor, S.J., Sweeney, C.M., Brereton, C.F., Lavelle, E.C., and Mills, K.H. (2009).
498 Interleukin-1 and IL-23 induce innate IL-17 production from gammadelta T cells, amplifying Th17
499 responses and autoimmunity. Immunity *31*, 331-341.
500
501 Torow, N., and Hornef, M.W. (2017). The Neonatal Window of Opportunity: Setting the Stage for
502 Life-Long Host-Microbial Interaction and Immune Homeostasis. J Immunol *198*, 557-563.
503
504 Tripathi, P., Kurtulus, S., Wojciechowski, S., Sholl, A., Hoebe, K., Morris, S.C., Finkelman, F.D.,
505 Grimes, H.L., and Hildeman, D.A. (2010). STAT5 is critical to maintain effector CD8+ T cell
506 responses. J Immunol *185*, 2116-2124.
507
508 Turchinovich, G., and Hayday, A.C. (2011). Skint-1 identifies a common molecular mechanism for
509 the development of interferon-gamma-secreting versus interleukin-17-secreting gammadelta T
510 cells. Immunity *35*, 59-68.
511
512 Villarino, A., Laurence, A., Robinson, G.W., Bonelli, M., Dema, B., Afzali, B., Shih, H.Y., Sun,
513 H.W., Brooks, S.R., Hennighausen, L.*, et al.* (2016). Signal transducer and activator of
514 transcription 5 (STAT5) paralog dose governs T cell effector and regulatory functions. eLife *5*.
515
516 Villarino, A.V., Sciume, G., Davis, F.P., Iwata, S., Zitti, B., Robinson, G.W., Hennighausen, L.,
517 Kanno, Y., and O'Shea, J.J. (2017). Subset- and tissue-defined STAT5 thresholds control
518 homeostasis and function of innate lymphoid cells. J Exp Med *214*, 2999-3014.
519
520 Wagatsuma, K., Tani-ichi, S., Liang, B., Shitara, S., Ishihara, K., Abe, M., Miyachi, H., Kitano, S.,
521 Hara, T., Nanno, M.*, et al.* (2015). STAT5 Orchestrates Local Epigenetic Changes for Chromatin
522 Accessibility and Rearrangements by Direct Binding to the TCRgamma Locus. J Immunol *195*,
523 1804-1814.
524
525 Wencker, M., Turchinovich, G., Di Marco Barros, R., Deban, L., Jandke, A., Cope, A., and Hayday,
526 A.C. (2014). Innate-like T cells straddle innate and adaptive immunity by altering antigen-receptor
527 responsiveness. Nat Immunol *15*, 80-87.
528
529 Wu, P., Wu, D., Ni, C., Ye, J., Chen, W., Hu, G., Wang, Z., Wang, C., Zhang, Z., Xia, W.*, et al.*
530 (2014). gammadeltaT17 cells promote the accumulation and expansion of myeloid-derived
531 suppressor cells in human colorectal cancer. Immunity *40*, 785-800.

532 Yao, Z., Cui, Y., Watford, W.T., Bream, J.H., Yamaoka, K., Hissong, B.D., Li, D., Durum, S.K.,
533 Jiang, Q., Bhandoola, A., *et al.* (2006). Stat5a/b are essential for normal lymphoid development
534 and differentiation. Proc Natl Acad Sci U S A *103*, 1000-1005.
535
536 Yao, Z., Kanno, Y., Kerenyi, M., Stephens, G., Durant, L., Watford, W.T., Laurence, A., Robinson,
537 G.W., Shevach, E.M., Moriggl, R., *et al.* (2007). Nonredundant roles for Stat5a/b in directly
538 regulating Foxp3. Blood *109*, 4368-4375.
539
540 Yu, F., Sharma, S., Edwards, J., Feigenbaum, L., and Zhu, J. (2015). Dynamic expression of
541 transcription factors T-bet and GATA-3 by regulatory T cells maintains immunotolerance. Nat
542 Immunol *16*, 197-206.
543
544 Zuberbuehler, M.K., Parker, M.E., Wheaton, J.D., Espinosa, J.R., Salzler, H.R., Park, E., and
545 Ciofani, M. (2019). The transcription factor c-Maf is essential for the commitment of IL-17-
546 producing gammadelta T cells. Nat Immunol *20*, 73-85.
547

548 **Acknowledgments**

556

557 **Author Contributions:** V.B. designed the study, oversaw all work, performed experiments and

558 wrote the manuscript. D.K. designed and performed experiments, analyzed data and helped write

559 the manuscript. J.R. and R.A. designed and performed experiments, analyzed data and helped

560 write the manuscript. H.N., T.S., B.M. and R.M. generated the STAT5 GOF mutant strains,

561 performed experiments, analyzed data and helped write the manuscript. E.C. and A.T. performed

562 and analyzed experiments.

563

564 **Competing interests:** The authors declare no competing interests.

565

566

567

Methods

Mice

All animal breeding and experiments were performed in house at DTU and only after approval from the Danish Animal Experiments Inspectorate. RORγt^{CRE} and RORγt^{GFP} mice (Lochner et al., 2008) were provided by Professor Gerard Eberl and subsequently bred in house. STAT5$^{F/F}$ mice were generated as previously described (Cui et al., 2004) and bred in house. STAT3$^{F/F}$ mice were purchased from The Jackson Laboratory and bred in house. RARdn$^{F/F}$ mice were generated as previously described (Rajaii et al., 2008), were provided by Professor William W. Agace, (Lund University, Sweden) and bred in house. Intestinal tissue from IL12$^{-/-}$ mice (JAX stock #002692) was provided by Professor William W. Agace, (Lund University, Sweden). GOF STAT5a and STAT5b mice were generated as previously described (Maurer et al., 2019; Pham et al., 2018) and were bred at the University of Veterinary Medicine Vienna (Vienna, Austria). Frozen sperm samples from Tbet-AmCyan mice (Yu et al., 2015) were provided by Professor Jinfang Zhu (NIH/NIAID, MD) and after re-derivation mice bred in house. Intestinal tissue from mice deficient in TRIF and MyD88 was provided by Dr Katharina Lahl (DTU, Denmark).

Cell culture media and buffers

All cell culture and single cell suspensions were prepared using RPMI 1640 (Invitrogen) supplemented with 10% heat inactivated fetal bovine serum (FBS)(Gibco), 20mM Hepes pH 7.4 (Gibco), 50 µM 2-mercaptoethanol, 2 mM L-glutamine (Gibco) and 10,000 U/ mL penicillin-streptomycin (Gibco). 10x Hank's balanced salt solution (HBSS)(Gibco) was diluted to 1x with sterile nuclease-free water and supplemented with 15 mM HEPES pH 7.4 (Gibco) to prepare HBSS-HEPES while it was supplemented with 2mM EDTA, 15mM HEPES, 50µg/mL Gentamycin and 2% FBS to prepare HBSS-EDTA. Isotonic Percoll was prepared by mixing 90%v/v of Percoll (GE healthcare) with 9%v/v 10x HBSS and 1%v/v 1M HEPES pH 7.4. Isotonic Percoll was subsequently diluted with HBSS-EDTA to the desired concentration. FACS buffer was prepared by mixing 3% heat inactivated FBS with DPBS (Gibco).

17

Isolation of lymphocytes from lymph nodes (LNs), thymus, skin, small intestine and colon

LNs were dissected, cleared off fat and crushed against a 70µm cell strainer to prepare single cell suspensions. Cell suspensions were then washed and filtered through a 40µm cell strainer. Cells were counted and 2.5×10^6 cells were used for staining of surface antigens and flow cytometry analysis.

Thymus lobes from 1-day old pups were dissected and dissociated in supplemented RPMI using dissection microscope to prepare single cell suspension. The cell suspensions were filtered through a 40µm cell strainer and stained for surface antigens under sterile conditions before FACS sorting.

Skin lymphocytes were prepared from ears as follows: first, the dorsal and ventral sides of the ears were mechanically separated, they were subsequently cut into small pieces followed by enzymatic digestion with 0.25mg/ml collagenase IV, 0.166mg/ml hyaluronidase and 0.1mg/ml DNase I (all enzymes from Sigma-Aldrich) in supplemented RPMI for 1 hour at 37°C with constant stirring at 700 rpm. Undigested tissue was crushed against a 70µm cell strainer to prepare a single cell suspension. After washing, the cell pellet was re-suspended and filtered through a 40µm cell strainer to remove tissue debris and used for flow cytometry staining.

Small intestines and colons were dissected from adult mice and were HBSS-HEPES to remove intestinal contents. Fat and Peyer's patches were removed before and then the tissues were open longitudinally and cut into small pieces of approximately 2-3 cm. Chopped tissue was washed 4 times (2 alternate cycles of 10 and 15 min each) using 15 mL of HBSS-EDTA buffer at 37°C in a shaking incubator. Tissue pieces were then digested using 0.3mg Liberase TM (Roche) and 0.15 mg of DNase (Sigma Aldrich) per preparation in 5mL supplemented RPMI for 40 minutes on the magnetic stirrer at 37°C. The resulting cell suspensions were filtered through 70µm cell strainers, collected in complete RPMI and subsequently pelleted by centrifugation. The cell pellets were then re-suspended in 5 mL 40% Percoll, layered on 4 mL of 70% Percoll, and centrifuged at 20 °C and 800 × g for 20 min with deceleration set to 0. Cells from the interphase were collected, washed once and then re-suspended in supplemented RPMI. For neonatal gut samples, cell

18

623   suspensions, following digestions, were filtered through 70µm cell strainers and were then used

624   directly.

625

Experimental Autoimmune Encephalomyelitis

627   EAE was induced by sub-cutaneous injection of 50µg of MOG35-55 peptide in CFA, while 2 ng

628   pertussis toxin were intra-peritoneally (i.p.) injected on the day of immunization and 2 days later.

629   From day 11 after immunization and until day 21, mice were weighed and scored for clinical signs

630   as follows: 0: no symptoms; 1: tail paralysis; 1.5: impaired righting reflex; 2: paralysis of one hind

631   limb; 2.5: paralysis of both hind limbs; 3: paralysis of one fore limb; 3.5: paralysis of one fore limb

632   and weak second for limb; 4: total limb paralysis.

633   Mice were euthanized at days 11 or 21 after immunization mice and were perfused with PBS.

634   LN cells were isolated as described above. Brain tissue was mechanically minced and passed

635   through a 70µm cell strainer to obtain a single cell suspension. Lymphocytes were separated using

636   density gradient centrifugation with 47% Percoll (GE Healthcare), layered on 4 mL of 70% Percoll,

637   and centrifuged at 20 °C and 900 × g for 30 min with deceleration set to 0.

638

***In vitro* stimulation of lymphocytes**

640   For LN lymphocytes, 10^7 cells were cultured for 3.5 hours in the presence of 50ng/ml PMA (Sigma)

641   ,750ng/ml ionomycin (Sigma) and 1µL /mL BD Golgistop (containing monensin). Single cell

642   suspensions from intestinal lamina propria were stimulated with 40 ng/ml of IL-23 (R&D Systems)

643   for 3 hours followed by 50ng/ml PMA, 750ng/ml ionomycin and 1µL /mL BD Golgistop for an

644   additional 3 hours. After 6 hours, cells were harvested and washed with PBS and used for flow

645   cytometry staining. FoxP3 transcription factor staining kit (eBiosciences)

646

Flow Cytometry

648   Cells were harvested by centrifugation at 400 g for 5 minutes at 4°C followed by staining with

649   fixable viability stain (BD Horizon FVS700) for 10 minutes on ice in PBS. Subsequently, surface

650   antigens were stained in FACS buffer for 30 minutes on ice. For cytokine staining, cells were then

19

651   fixed and permeabilized by incubation in BD Fix/Perm solution for 15 minutes at room temperature

652   followed by washing once in BD Perm/Wash solution. Intracellular cytokines were stained in BD

653   Perm/Wash for 15 minutes at room temperature. For transcription factor staining, following surface

654   staining, the cells were fixed using the Fixation/Permeabilization buffer in BD Transcription Factor

655   kit for 45 minutes at 4^oC. Transcription factors were stained in permeabilization buffer from the

656   same kit for 45 minutes at 4^oC. Conversely, for combined transcription factor and cytokine staining,

657   after surface staining, the cells were fixed using the Fixation/Permeabilization buffer in FoxP3

658   transcription factor staining kit (eBiosciences) for 1 hour at 4^oC. Cytokines and transcription factors

659   were then stained in the permeabilization buffer from the same kit following the manufacturer's

660   guidelines.

661   All antibodies were used at a 1:200 dilution unless otherwise specified. Antibodies used herein

662   were as follows: CD4-FITC (RM4-4,BD biosciences), CD19-FITC (6D5,Biolegend), TCRβ-

663   APCeF780 (H57-597; eBioscience), TCRγδ-BV421 (GL3,BD biosciences), CD45-V500 (30-F11,

664   BD biosciences), CD3-PECF594 (BM10-37, BD biosciences), RORγt-APC (B2D, BD biosciences),

665   IL-17-BV786 (TC11-18H10, BD biosciences), IL-22-PE (1H8PWSR; eBioscience), T-bet-PECy7

666   (4B10,Biolegend), IFNγ-PerCP-Cy5.5 (XMG1.2; BD biosciences), CD69-V450 and Pe-CF594

667   (H1.2F3; BD biosciences), CCR6-Alexa Fluor 647 (140706; BD biosciences), CD27 PE-Cy7

668   (LG.3A10; BD biosciences), CD44-V500 (1M7; BD biosciences), Ki67-BV786 (B56 ; BD

669   biosciences 1:100)

670   To determine the level ofpSTAT5, $1x10^6$ cells were fixed 100 µL with BD phosflow Lyse/Fix

671   (diluted to 1x with water) for 10 minutes at 37^oC.Subsequently, cells were washed once with FACS

672   buffer and re-suspended in 100 µL BD phosflow perm buffer III, which was pre-chilled to -20^oC,

673   and incubated on ice for 30 minutes. Cells were then washed once with FACS buffer and stained

674   for 30 minutes on ice in FACS buffer. Antibodies used in the staining of p-STAT5 were: CD4-FITC

675   (GK1.5; BD Biosciences), CD8-APC 53-6.7; BD Biosciences) and pSTAT5-PEcy7 (47/Stat5

676   pY694; BD Biosciences; 5 µL/test). Samples were acquired using BD LSR Fortessa™ and BD

677   FACSDiva software v8.0.2.

678

Bone Marrow chimera

First, $CD45.1^+CD45.2^+$ mice were lethally irradiated (900 rad). Next day they were injected

intravenously with 10×10^6 cells of whole bone marrow cells from $CD45.1^+$ wild-type and $CD45.2^+$

$ROR\gamma t^{CRE}$-$STAT5^{F/F}$ mixed at 1:1 ratio. All Chimeras were analyzed after 12-14 weeks after

reconstitution.

Antibiotics administration

Pregnant female mice were treated with a cocktail of the following antibiotics: 1mg/ml Collistin, 5

mg/ml Streptomycin, 1mg/ml Ampicillin and 0.5mg/ml Vancomycin (all antibiotics Sigma) in their

drinking water starting three days before delivery and until weaning of pups (3 weeks after the

birth). The antibiotic-containing drinking water was replaced once a week until analysis.

Citrobacter infection

Citrobacter. rodentium strain DBS100 (ATCC 51459; American Type Culture Collection) was

purchased from ATCC and was cultured in Luria–Bertani broth overnight. CFU/ml (Dose) was

determined by measuring the OD at 600 nm. Pups that were 10-12 days old were infected by oral

gavage of 5×10^6 CFU/mouse in a volume of 50µl. At day 6 post infection, the pups were

euthanized and colons and fecal samples were collected. Bacterial load in the feces was

determined as described (Sagaidak et al., 2016).

Cell sorting, RNA extraction, cDNA synthesis and Real-Time PCR

Stained cells from thymi of 1-day old pups were sorted using BD ARIA FUSION™ and BD

FACSDiva software v8.0.2. Target populations were sorted directly in RLT buffer (Qiagen)

supplemented with 2-mercaptoethanol. Total RNA was extracted using Rneasy micro kit (Qiagen)

and then used for cDNA synthesis using iScript cDNA synthesis kit (Biorad), according to the

manufacturer's protocol. SsoFast EvaGreen supermix (Biorad) was used to catalyze real-time PCR

reactions, which were run on CFX96 (Biorad) and analyzed using Bio-rad CFX manager software.

Gene expression levels were normalized to that of beta-actin. The following primers were used:

21

707   *Actb*, Fwd-GGCTGTATTCCCCTCCATCG, Rev- CCAGTTGGTAACAATGCCATGT; *Stat5a*, Fwd-

708   TCCGCAGCACCAGGTAAA, Rev- GGGATTATCCAAGTCAATAGCATC; *Stat5b*, Fwd-

709   ACAACGGCAGCTCTCCAG, Rev-TGGGCAAACTGAGCTTGGATC.

710

711   **Data Analysis**

712   Flow cytometry data was analyzed using Flow Jo V 10 software. All the statistical analyses and

713   graphs were generated using Prism v7. All statistical tests used are described in the Figure
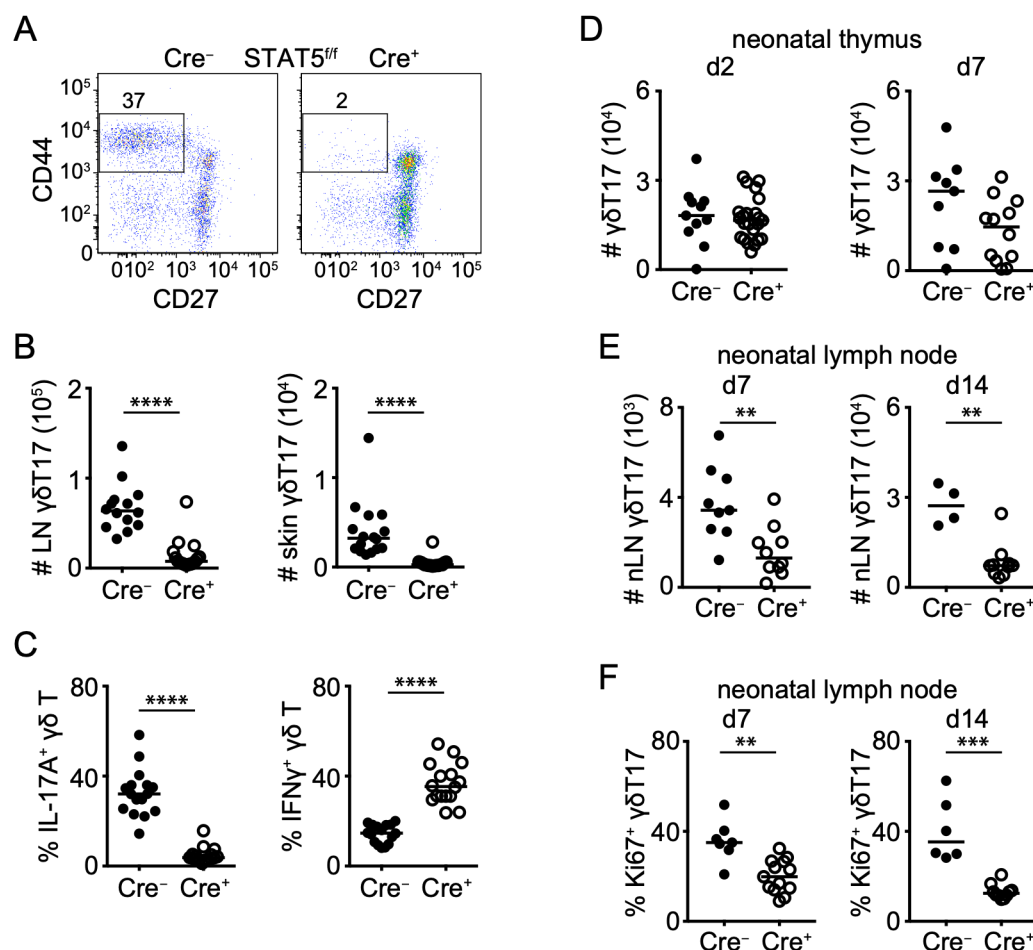
714   legends

715

716

717 **Figures and Legends**

718 **Figure 1**

719 **Figure 1. STAT5 is necessary for the neonatal expansion of γδT17 cells**

720 Flow cytometric analysis of γδ T cells in RORγt[CRE]-STAT5[F/F] (Cre[+]) and littermate control mice

721 (Cre[-]). In graphs each symbol represents a mouse and line the median. **p < 0.01, ***p < 0.001,

722 ****p < 0.0001 using Mann-Whitney test.

723 (A) Expression of CD27 and CD44 in order to identify CD27^{-}CD44^{+} γδT17 cells in the LN.

724 Numbers indicate percent of CD27^{-}CD44^{+} within the γδ T cell compartment.

725 (B) Numbers of γδT17 cells in the LN (staining as in A) and skin. In the skin, γδT17 cells were

726 identified as CD45^{+}CD3[Low]Vγ5^{-}TCRβ^{-}TCRγδ^{+}CCR6^{+}.

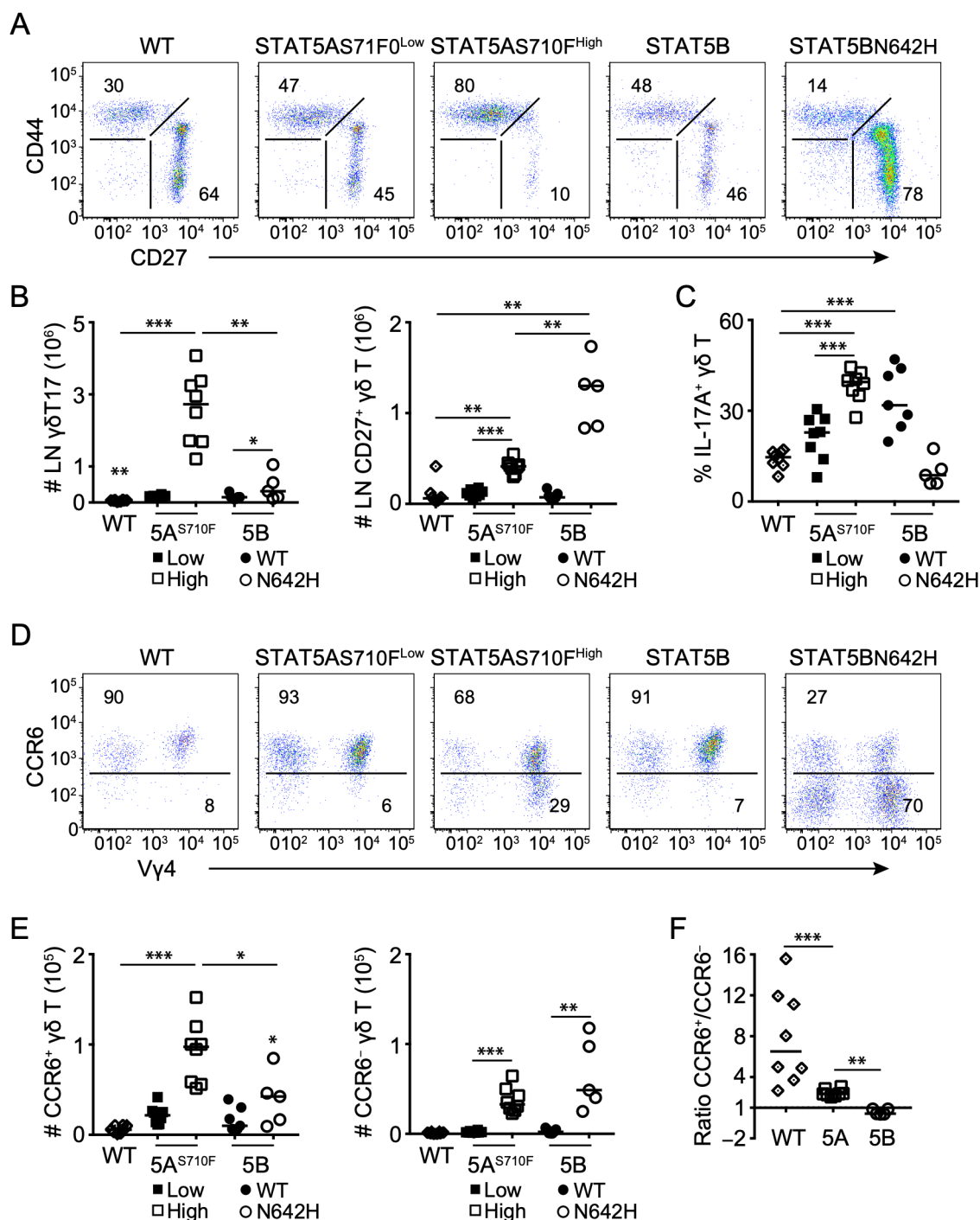727 (C) Expression of IL-17A and IFNγ within the LN γδ T cell compartment.

728 (D) Numbers of CD27^{-}CD44^{+} γδT17 cells in day 2 and day 7 old thymi.

729 (E) Numbers of CD27^{-}CD44^{+} γδT17 cells in day 7 and day 14 old LN.

730   (F) Frequency of Ki67$^+$RORγt$^+$ or Ki67$^+$CCR6$^+$ $\gamma\delta$T17 cells within the CD44$^+$TCR$\gamma\delta^+$ compartment

731   in day 7 and day 14 old LN.

732

733

734 **Figure 2**

735 **Figure 2. Differential impact of STAT5A and STAT5B on γδT17 and CD27⁺ γδ T cells**

736 Flow cytometric analysis of γδ T cells in mice that are either wild-type (WT) or constitutively

737 express under the *Vav1* promoter one of the following forms of STAT5: low (STAT5AS710F^{Low}) or

738 high (STAT5AS710F^{High}) copy number of the hyperactive STAT5A S710F mutant, or human wild-

739 type (STAT5B) or the hyperactive N642H STAT5B mutant (STAT5BN642H). In graphs, each

740   symbol represents a mouse and line the median. *p < 0.05, **p < 0.01, ***p < 0.001 using Mann-

741   Whitney test.

742   (A) Expression of CD27 and CD44 in order to identify CD27$^-$CD44$^+$ γδT17 cells in the LN.

743   Numbers indicate percent of CD27$^-$CD44$^+$ or CD27$^+$CD44$^-$ within the γδ T cell compartment.

744   (B) Numbers of γδT17 (staining as in A) and CD27$^+$ cells in the LN (** in WT denotes difference by

745   comparison to STAT5BN642H).

746   (C) Expression of IL-17A within the LN γδ T cell compartment.

747   (D) Expression of CCR6 and Vγ4 in skin γδT17 cells (staining as in Fig. 1B). Numbers indicate

748   percent of CCR6$^+$ or CCR6$^-$ cells within the γδ T cell compartment.

749   (E) Numbers of CCR6$^+$ and CCR6$^-$ cells identified in D (* in STATBBN642H denotes significant

750   difference by comparison to WT). (F) Ratio of CCR6$^+$ over CCR6$^-$ cells in WT compared to

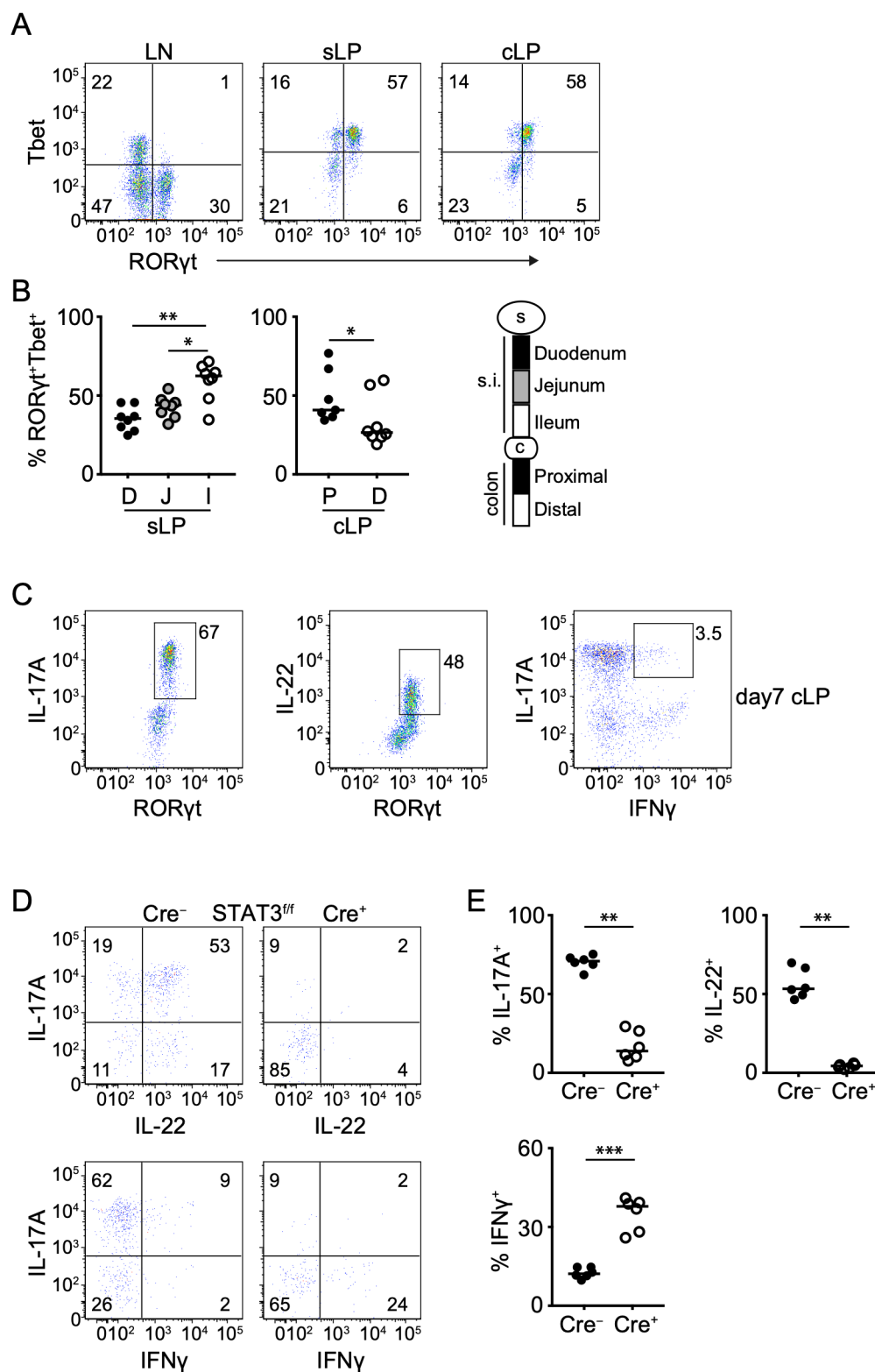751   STAT5AS710F^{High} (5A) and STAT5BN642H (5B) mice.

752

753

26

Figure 3

Figure 3. RORγt^{CRE}-STAT5$^{F/F}$ mice are resistant to EAE

Disease progression and flow cytometric analysis of γδ and CD4$^+$ T cells in RORγt^{CRE}-STAT5$^{F/F}$ (Cre$^+$) and littermate control mice (Cre$^-$) that had been previously immunized with 50 µg MOG peptide in CFA and 200 ng Pertussis toxin. In graphs, each symbol represents a mouse and line the median (except in A). **p < 0.01, ***p < 0.001, ****p < 0.0001 using Mann-Whitney test.

(A) Clinical symptoms of EAE until day 21 post immunization. Data is pool of 20 mice per genotype and shown as mean±sem. Statistical analysis was performed using 2-way ANOVA with Bonferroni's multiple comparisons test. ANOVA p-value < 0.0001; Bonferroni's test returned significance for days 11-21 with day 11 p = 0.003 and days 12-21 p < 0.0001.

(B-C) Numbers of γδT17 cells in the LN (staining as in Fig. 1A) of unimmunized controls (EAE$^-$) and at 11 (B) and 21 (C) days after immunization.

(D) Numbers of γδT17 cells in the brain (identified as CD45$^+$CD3$^+$TCRβ$^-$TCRγδ$^+$CD44$^+$) at days 11 and 21 after immunization.

(E) Expression of IL-17A within the LN γδ T cell compartment of unimmunized controls (EAE$^-$) and at 11 and 21 days after immunization. (F) Numbers of CD4$^+$CD44$^+$CD3$^+$TCRβ$^+$ cells in the brain at days 11 and 21 after immunization.

27

772 **Figure 4**

773 **Figure 4. Intestinal γδT17 cells express Tbet and require STAT3 for IL-17A and IL-22**

774 Flow cytometric analysis of LN and intestinal γδ T cells in WT or in RORγt^{CRE}-STAT3$^{F/F}$ (Cre$^+$) and

775 littermate control mice (Cre$^-$). In graphs, each symbol represents a mouse and line the median.

776   Cytokine detection was performed following IL-23 re-stimulation. *p < 0.05, **p < 0.01, ***p <

777   0.001, ****p < 0.0001 using Mann-Whitney test.

778   (A) Expression of RORγt and Tbet within the γδ T cell compartment of the LN, sLP and cLP.

779   Numbers indicate percent of RORγt and Tbet expression.

780   (B) Frequency of RORγt$^+$Tbet$^+$ cells within the γδ T cell compartment in the indicated small

781   intestinal and colonic segments.

782   (C) Expression of RORγt and IL-17A, RORγt and IL-22, or IL-17A and IFNγ in the γδ T cell

783   compartment of cLP from day 7 old mice (representative of two experiments).

784   (D) Expression of IL-17A and IL-22 (top) or IL-17A and IFNγ (bottom) in RORγt^{CRE}-STAT3$^{F/F}$ (Cre$^+$)

785   and littermate control mice (Cre$^-$). Numbers indicate percent of positive expression.

786   (E) Frequency of IL-17A$^+$, IL-22$^+$ and IFNγ$^+$ γδ T cells in RORγt^{CRE}-STAT3$^{F/F}$ (Cre$^+$) and littermate

787   control mice (Cre$^-$).
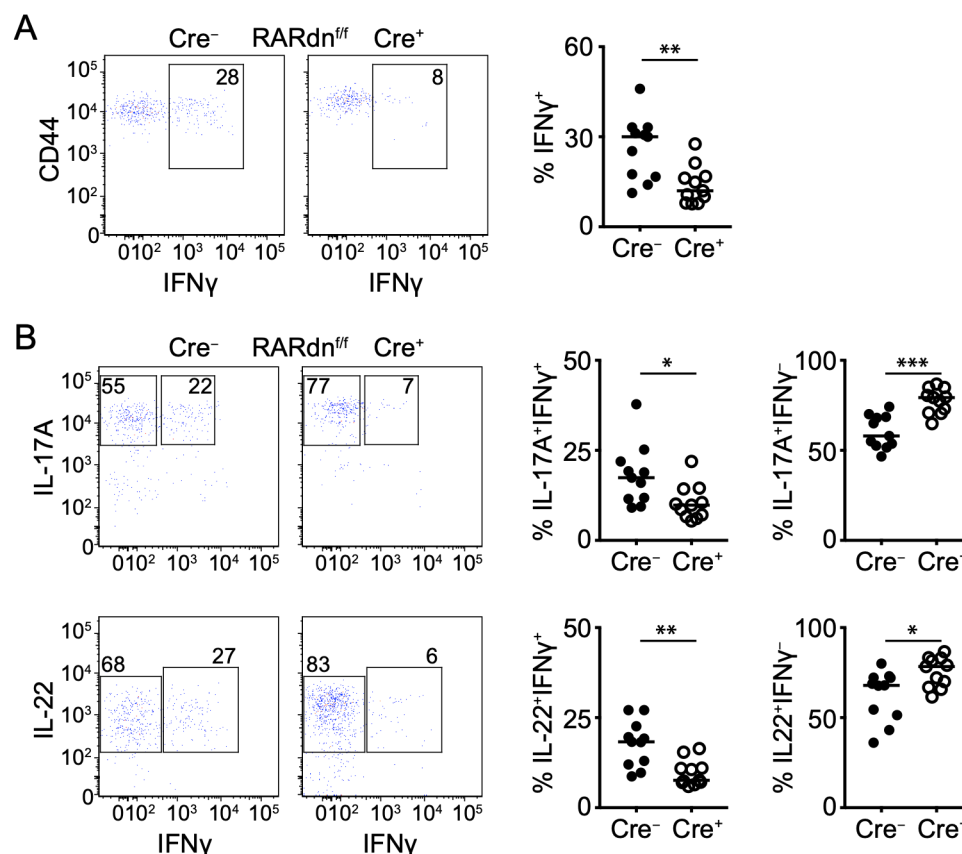
788

789

29

Figure 5

Figure 5. Retinoic acid receptor signaling regulates IFNγ production in intestinal Tbet⁺ γδT17 cells

Flow cytometric analysis of cytokine expression in colonic γδ T cells in RORγt^CRE-RARdn^F/F (Cre⁺) and littermate control mice (Cre⁻) following IL-23 stimulation. In graphs, each symbol represents a mouse and line the median. *p < 0.05, **p < 0.01, ***p < 0.001 using Mann-Whitney test.

(A) Expression of CD44 and IFNγ (dot plots) and frequency of IFNγ ⁺ γδ T cells (graph) in RORγt^CRE-RARdn^F/F (Cre⁺) and littermate control mice (Cre⁻).

(B) Expression of IL-17A and IFNγ (top dot plots) or IL-22 and IFNγ (bottom dot plots) with graphical representation of the frequency of IL-17A⁺IFNγ⁺ and IL-17A⁺IFNγ⁻ or IL-22⁺IFNγ⁺ and IL-22⁺IFNγ⁻ γδ T cells in RORγt^CRE-RARdn^F/F (Cre⁺) and littermate control mice (Cre⁻).

30

803   **Figure 6**
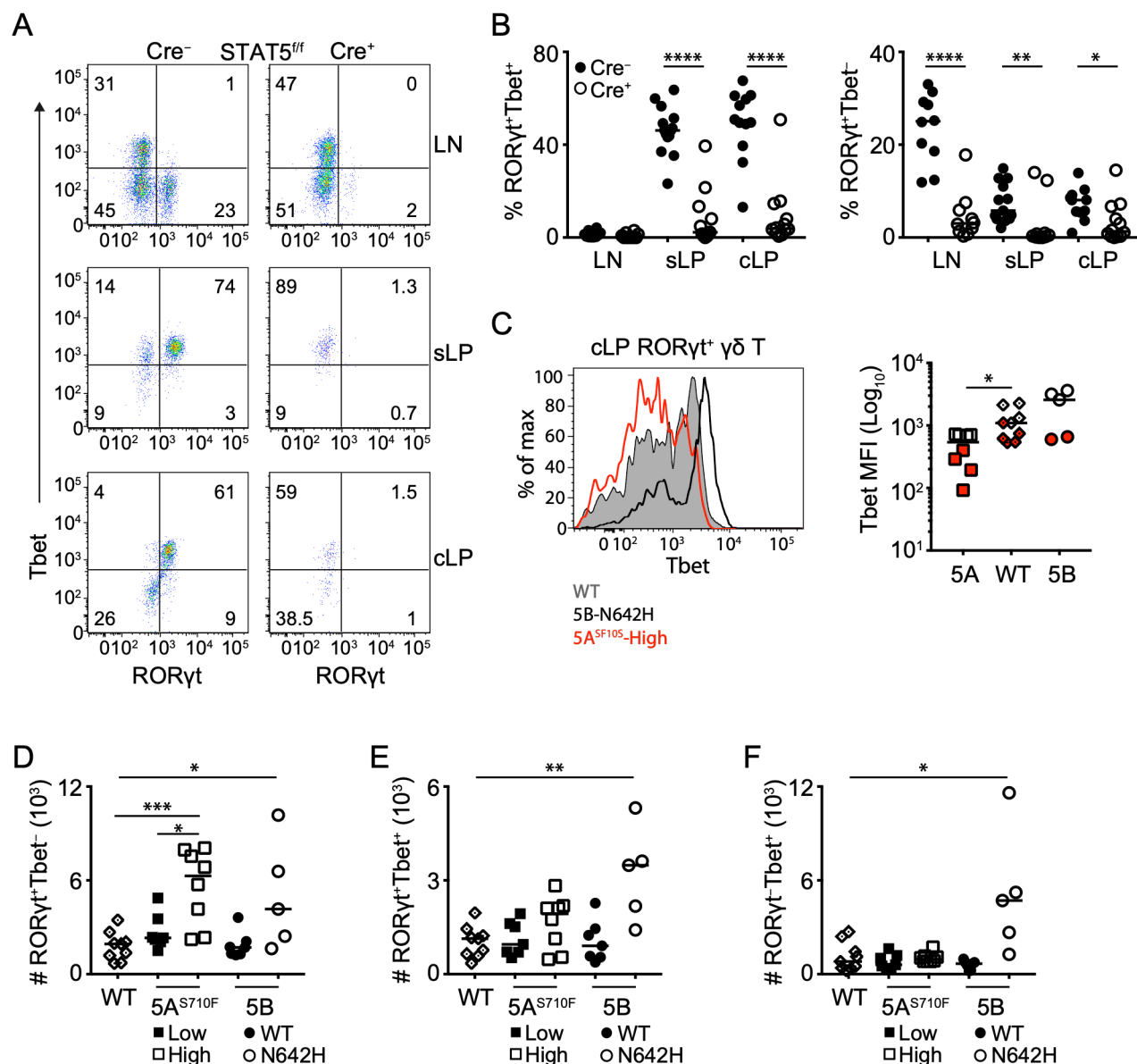
804   **Figure 6. STAT5 is a critical determinant of Tbet-expressing intestinal γδT17**

805   Flow cytometric analysis of intestinal γδ T cells in RORγt^{CRE}-STAT5$^{F/F}$ (Cre$^+$) and littermate control

806   mice (Cre$^-$) in STAT5A and STAT5B hyperactive mutant mice as described in Figure 2. In graphs,

807   each symbol represents a mouse and line the median. *p < 0.05, **p < 0.01, ***p < 0.001, ****p <

808   0.0001 using Mann-Whitney test.

809   (A) Expression of RORγt and Tbet within the γδ T cell compartment of the LN, sLP and cLP.

810   Numbers indicate percent of RORγt and Tbet expression.

811 (B) Frequency of RORγt$^+$Tbet$^+$ and RORγt$^+$Tbet$^-$ cells within the γδ T cell compartment in LN, sLP

812 and cLP.

813 (C) Expression of Tbet (histogram) and Tbet mean fluorescent intensity (MFI) (graph) in RORγt$^+$

814 cLP γδ T cells from WT, STAT5AS710F^{High} (5a) or STAT5BN642H (5b) mice as described in

815 Figure 2. In graph, colors indicate two different experiments.

816 (D) Numbers of RORγt$^+$ (E), RORγt$^+$Tbet$^+$ (F) and RORγt$^-$Tbet$^+$ γδ T cells in the cLP of the

817 indicated STAT5A and STAT5B hyperactive mutant mice or WT control mice.

818
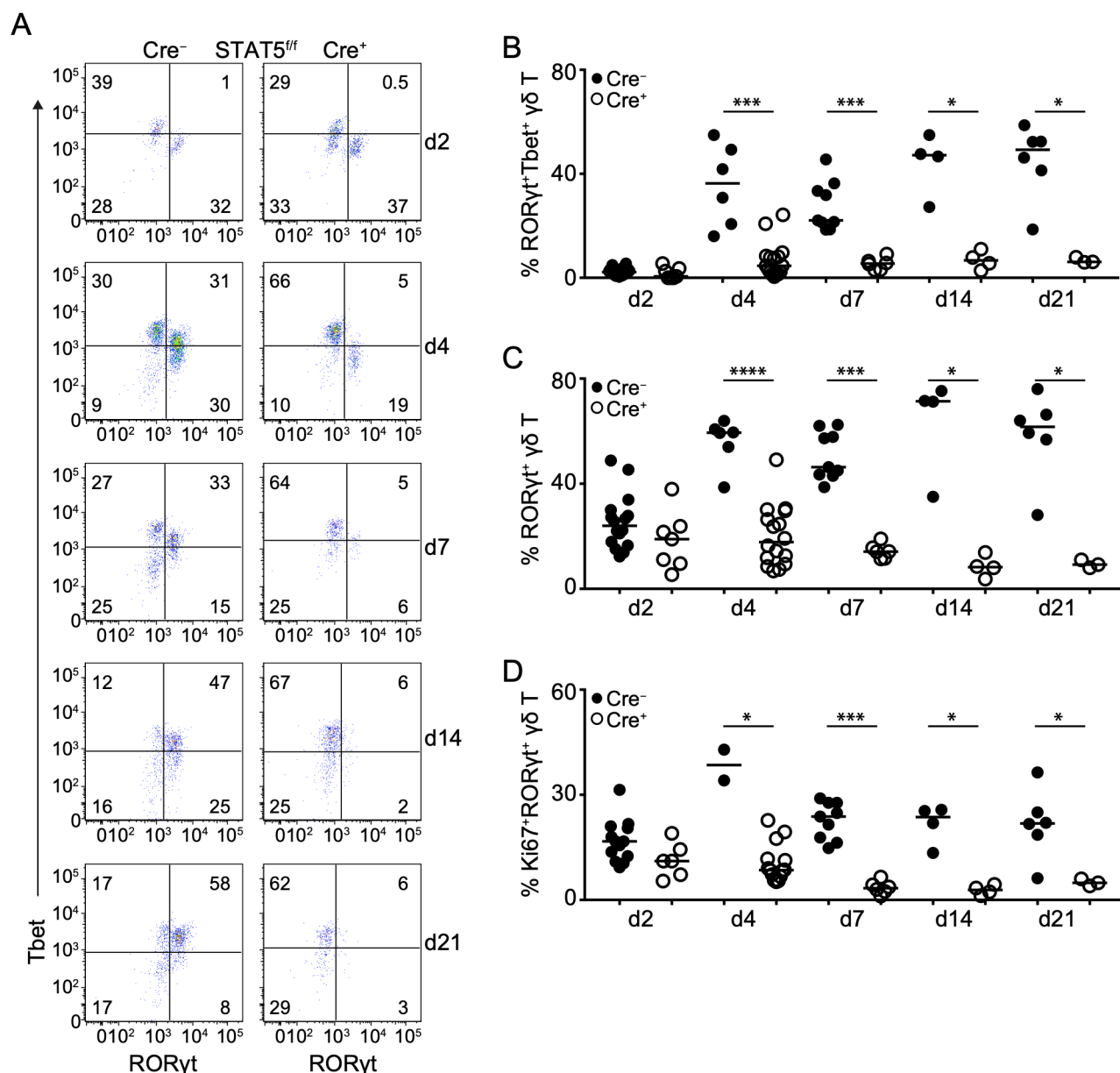
Figure 7

820 **Figure 7. STAT5 regulates the neonatal fate of intestinal Tbet$^+$ γδT17 cells**

821 Flow cytometric analysis of colonic γδ T cells in RORγt^{CRE}-STAT5$^{F/F}$ (Cre$^+$) and littermate control

822 mice (Cre$^-$) during neonatal ontogeny. Day of birth is counted as day(d)1. In graphs each symbol

823 represents a mouse and line the median. *p < 0.05, **p < 0.01, ***p < 0.001, ****p < 0.0001 using

824 Mann-Whitney test.

825 (A) Expression of RORγt and Tbet within the γδ T cell compartment of cLP at the indicated days

826 after birth. Numbers indicate percent of RORγt and Tbet expression.

827 (B) Frequency of cLP RORγt$^+$Tbet$^+$ γδ T cells at the indicated days after birth.

828   (C) Frequency of cLP RORγt$^+$ γδ T cells (including Tbet$^+$) at the indicated days after birth.

829   (D) Frequency of cLP Ki67$^+$RORγt$^+$ γδ T cells at the indicated days after birth.

830

831